IOP Conf. Series: Journal of Physics: Conf. Series **1256** (2019) 012006 doi:10.1088/1742-6596/1256/1/012006

Comparison of Analytical Wake Models with Wind Tunnel Data

F Campagnolo[1], A Molder[1], J Schreiber[1], C L Bottasso[1]

[1] Wind Energy Institute, Technische Universität München, Boltzmannstraße 15, D-85748 Garching bei München, Germany

E-mail: {filippo.campagnolo, anil.molder, johannes.schreiber, carlo.bottasso}@tum.de

Abstract. In this paper a comparison between the wake velocity, wake deflection and turbulence intensity predictions of several wake models was carried out against wind tunnel data obtained with a state-of-the-art scaled wind turbine model. In order to achieve a fair comparison, the models' parameters were all tuned with respect to the same experimental data-set using the Maximum Likelihood Estimation (MLE) method. A quantitative assessment of all models' predictions highlighted that the Porté-Agel model seems to provide, for a wide range of inflow and wind turbine operating conditions, the most accurate estimation of the wake flow field. Further improvements to the model are also suggested in the conclusions.

1. Introduction

In recent years, many research activities have focused on formulating cooperative control strategies for wind turbines that aim at maximizing the power produced by a wind farm. Among the developed strategies, the ones that showed so far the greatest potential are based on de-rating or misaligning, with respect to the wind, the upstream wind turbines [1]. In this regard, many research institutes have developed analytical models to predict the effects that these strategies have on the wake shed by a wind turbine. Many of these models require the calibration of tuning parameters, an activity that implies the availability of experimental data, often obtained through wind tunnel tests, or data obtained by means of CFD simulations. However, the data set used for the calibration of the various models is often heterogeneous: experimental/numerical data, different inflow conditions, different characteristics and operating conditions of the used wind turbine models. All this hampers an objective and quantitative comparison of the accuracy of these models, whose calibration parameters are often optimized for a specific inflow or wind turbine operating condition. This article therefore aims at comparing the prediction of different analytical wake models with data obtained by testing a state-of-the-art wind turbine scaled model in a boundary layer wind tunnel. To this end, and in order to ensure a fair comparison, the models' parameters are all re-tuned using the data itself. This paper is therefore organized as following: at first an overview of the investigated analytical wake models, including the related equations and tunable parameters, is provided in §2. Next, the experimental setup is presented in §3, followed by the description of the approach adopted for the tuning of the parameters, given in §4. Successively, the comparison between the models' predictions and the experimental data is discussed in §5, while the conclusions are drawn in §6.

2. Overview of analytical wake models

2.1. Jensen wake model

The Jensen one-dimensional wake model proposed in [2] is a pioneering work in the field. It assumes a top hat shape of the velocity $U(x)$ within the wake by means of Eq. 1, where the tunable parameter α governs the wake recovery, U_0 is the inflow speed, D_0 is the rotor diameter, x is the downstream distance to the rotor disk and a the rotor axial induction.

$$U(x) = U_0 \left\{ 1 - 2a \left(\frac{D_0}{D_0 + 2\boldsymbol{\alpha} x} \right)^2 \right\}. \tag{1}$$

2.2. Frandsen wake model

The Frandsen [3] wake model also estimates the flow velocity in the wake assuming a top hat shape distribution. Differently than the Jensen model, the wake diameter $D(x)$ and wake expansion coefficient $\alpha(x)$ are calculated as

$$\frac{U(x)}{U_0} = \frac{1}{2} + \frac{1}{2}\sqrt{1 - 2\frac{D_0^2}{D(x)^2}C_T}, \quad \text{with } \frac{D(x)}{D_0} = (\beta^{\boldsymbol{k}/2} + \alpha s)^{1/\boldsymbol{k}}, \tag{2a}$$

$$\alpha(x) = \beta^{\boldsymbol{k}/2}[(1 + 2\boldsymbol{\alpha_{(noj)}} s)^{\boldsymbol{k}} - 1]s^{-1}, \quad \text{with } \beta = \frac{1}{2}\frac{1 + \sqrt{1 - C_T}}{\sqrt{1 - C_T}}, \tag{2b}$$

with $s = x/D_0$ and C_T the rotor thrust coefficient, while $\alpha_{(noj)}$ and are k are the tunable parameters that govern the wake recovery.

2.3. FLORIS wake model

The FLOw Redirection and Induction in Steady-state (FLORIS) wake model [4] considers the flow within the wake as the superimposition of three wake zones, each characterized by an expansion and decay rates governed by different coefficients, denoted with subscript q in Eqs. 3, in turn function of tunable parameters $m_{e,q}$, $M_{U,q}$, a_U and b_U. The model is also capable of predicting the wake lateral displacement $y_{w,yaw}(x)$ associated to a rotor that operates misaligned, of an angle γ, with respect to the wind direction, as shown in Eqs. 3c-3d, where k_d is a tunable parameter. The overall wake lateral displacement from the rotor centerline $y_w(x)$ also accounts for the combined effect of rotor rotation and wind shear, as shown in Eq. 3e, with a_d and b_d being tunable parameters.

$$D_q(x) = \max(D_0 + 2k_e \boldsymbol{m_{e,q}} x, 0), \tag{3a}$$

$$U(x,r) = U_0[1 - 2ac(x,r)], \quad \text{with } c(x,r) \text{ function of } c_q(x) = \left[\frac{D_0}{D_0 + 2k_e m_{U,q}(\gamma) x} \right]^2, \tag{3b}$$

$$m_{U,q}(\gamma) = \frac{\boldsymbol{M_{U,q}}}{\cos(\boldsymbol{a_U} + \boldsymbol{b_U}\gamma)}, \tag{3c}$$

$$y_{w,yaw}(x) \approx \frac{\tilde{C_T}(a,\gamma)\left[15\left[\frac{2x\boldsymbol{k_d}}{D_0} + 1\right]^4 + \tilde{C_T}(a,\gamma)^2\right]}{\frac{30\boldsymbol{k_d}}{D_0}\left[\frac{2x\boldsymbol{k_d}}{D_0} + 1\right]^5}, \tag{3d}$$

$$y_w(x) = y_{w,rot}(x) + y_{w,yaw}(x), \quad \text{with } y_{w,rot}(x) = \boldsymbol{a_d} + \boldsymbol{b_d} x. \tag{3e}$$

2.4. Porté-Agel wake model

The Porté-Agel wake model was firstly proposed in [9], further improved in [10] and presented in its final form in [11]. The model is capable of computing the relative wake deficit $\Delta U/U_0$ in a 3-D domain using Eqs. 4a-4c, where the wake decay rate depends, through the tunable parameters k_a and k_b, to the inflow turbulence intensity. The wake deflection δ associated to misaligned condition is computed with Eq. 4e, which accounts for the the deflection in the near and far wake. The first one is governed by the wake skew angle at the rotor disk θ_{C_0} and by the length of the wake potential core x_0, which is a function of two tunable parameters α^* and β^*. The wake turbulence intensity is calculated with the model proposed in [12] (Eq. 4g), where $TI_{a,b,c,d}$ are tunable parameters.

$$\frac{\Delta U(x,y,x)}{U_0} = \left(1 - \sqrt{1 - \frac{C_T \cos\gamma}{8(\sigma_y \sigma_z / {D_0}^2)}}\right) \exp\left(-0.5\left(\frac{y-\delta}{\sigma_y}\right)^2\right) \exp\left(-0.5\left(\frac{z-z_h}{\sigma_z}\right)^2\right), \tag{4a}$$

$$\frac{\sigma_y(x,\gamma)}{D_0} = k_y \frac{(x-x_0)}{D_0} + \frac{\cos\gamma}{\sqrt{8}} \quad \text{and} \quad \frac{\sigma_z(x)}{D_0} = k_z \frac{(x-x_0)}{D_0} + \frac{1}{\sqrt{8}}, \tag{4b}$$

$$k_y = k_z = \boldsymbol{k_a} I_0 + \boldsymbol{k_b}, \tag{4c}$$

$$\frac{x_0(I_0,\gamma)}{D_0} = \frac{\cos\gamma(1+\sqrt{1-C_T})}{\sqrt{2}(\boldsymbol{\alpha^*} I_0 + \boldsymbol{\beta^*}(1-\sqrt{1-C_T}))}, \tag{4d}$$

$$\frac{\delta}{D_0} = \theta_{C_0}\frac{x_0}{D_0} + \frac{\theta_{C_0}}{14.7}\sqrt{\frac{\cos\gamma}{k_y k_z C_T}}(2.9 + 1.3\sqrt{1-C_T} - C_T)\ln\left[\frac{(1.6+\sqrt{C_T})\left(1.6\sqrt{\frac{8\sigma_y\sigma_z}{{D_0}^2\cos\gamma}} - \sqrt{C_T}\right)}{(1.6-\sqrt{C_T})\left(1.6\sqrt{\frac{8\sigma_y\sigma_z}{{D_0}^2\cos\gamma}} + \sqrt{C_T}\right)}\right], \tag{4e}$$

$$\theta_{C_0}(\gamma) = \frac{0.3\gamma}{\cos\gamma}(1 - \sqrt{1 - C_T\cos\gamma}), \tag{4f}$$

$$I_{wake}^2 = \sqrt{I_0^2 + I_+^2}, \quad \text{with } I_+(I_0,x) = \boldsymbol{TI_a} a^{\boldsymbol{TI_b}} I_0^{\boldsymbol{TI_c}} (x/D_0)^{\boldsymbol{TI_d}}. \tag{4g}$$

2.5. 2D_k Jensen wake model

The 2D_k Jensen wake model, proposed in [5] and improved in [6], provides equations for modeling the flow velocity and turbulence intensity within the wake. At first the one-dimensional flow velocity is computed using a wake decay coefficient that is proportional, through the tunable parameter k_0, to both the inflow (I_0) and wake turbulence intensity. The turbulence within the wake is then predicted with the Larsen model [7] (Eq. 5b), where $TI_{a,b}$ are tunable parameters. The 2-D velocity deficit is then approximated by a cosine function (Eq. 5c).

$$u^*(x) = U_0\left[1 - \frac{1-\sqrt{1-C_T}}{\left(1+\frac{kx}{D_0/2}\right)^2}\right], \quad \text{with } k = \boldsymbol{k_0}\frac{I_{wake}}{I_0}, \tag{5a}$$

$$I_{wake} = \sqrt{I_0^2 + I_{add}^2}, \quad \text{with } I_{add}(x) = \boldsymbol{TI_a}(x/D_0)^{\boldsymbol{TI_b}}\sqrt{1-\sqrt{1-C_T}}, \tag{5b}$$

$$U(x,r) = (U_0 - u^*(x))\cos\left(\frac{\pi}{r_x}r + \pi\right) + u^*(x), \quad \text{with } r_x = kx + \frac{D_0}{2}. \tag{5c}$$

2.6. Jensen-Gaussian wake model
The Jensen-Gaussian wake model [8] is similar to the previous 2D_k Jensen. The one-dimensional flow velocity is calculated first through the tunable parameters k_0 and K_n, with K_n also affecting the turbulence intensity in the wake, while the velocity distribution, assumed Gaussian, is calculated according to Eq. 6b:

$$u^*(x) = u_0 \left[1 - \frac{2a}{\left(1 + \frac{kx}{r_1}\right)^2}\right], \quad \text{with } k = \boldsymbol{k_0}\frac{I_{wake}}{I_0},\ I_{wake}(x) = \left(\boldsymbol{K_n}\frac{C_T}{(x/D)^{0.5}} + I_0^{0.5}\right), \tag{6a}$$

$$U(x,r) = U_0 - (u_0 - u^*)\frac{5.16}{\sqrt{2\pi}} e^{\frac{-r^2}{2(r_x/2.58)^2}}, \quad \text{with } r_x = kx + r_1 \text{ and } r_1 = \frac{D_0}{2}\sqrt{\frac{(1-a)}{(1-2a)}}. \tag{6b}$$

3. Experimental setup
The experimental data were obtained by means of wind tunnel testing. In detail, experiments were conducted in the boundary-layer test section of the Politecnico di Milano wind tunnel using a scaled G1 wind turbine [13]. Two different inflows were simulated: one characterized by a moderate turbulence intensity (mod-TI) equal to 6.1%, and one characterized by high turbulence intensity (high-TI), equal to 11%. The mean undisturbed wind speed, measured at hub height with a pitot tube placed 5D upstream of the G1, was 5.60 and 5.46 m/s, respectively for mod-TI and high-TI inflow.

For both inflows, 11 experimental observations were conducted, each one characterized by a different wind turbine operating condition. Nine observations were performed with the rotor disk misaligned of $\gamma = -40° : 10° : +40°$ with respect to the wind tunnel axis (positive misalignment corresponds to a counter-clockwise rotation from the wind to the rotor axis looking down onto the terrain), while two observations where conducted with the the aligned G1 operated under power de-rating conditions. During each test, a closed-loop wind turbine controller [13] was used to find the optimal rotational speed Ω and collective blade pitch β. Their average values are reported in Table 1 together with the rotor thrust coefficient C_T. These were computed by means of a Blade Element Momentum (BEM) model that makes use of tuned airfoil polars [14], and were extremely close to the thrust coefficients computed using the fore-aft load sensor placed at tower base.

The speed in the wake was measured, at 5D, 7.5D and 10D downwind of the G1, using a hot-wire traversing system [15] and along horizontal lines at hub height, thus generating a total of 66 data sets.

4. Formulation of the tuning method
From the the experimental data-set, average normalized flow velocities and turbulence intensities were derived at specific locations expressed in Cartesian coordinates (x, y, z). To account for the inhomogeneity of the flow within the wind tunnel [16], the normalized flow velocities were obtained by dividing the average speed in the wake by the corresponding velocity previously measured at the same coordinate (y, z), but three diameters upstream of the model. In this work, the model outputs $\hat{\boldsymbol{y}}^i$, associated to the i^{th} experimental observation $\tilde{\boldsymbol{y}}^i$, are therefore defined as

$$\hat{\boldsymbol{y}}^i = \left[\ldots, \left(\hat{\boldsymbol{v}}^{i,d}\right)^T, \left(\hat{\boldsymbol{t}}^{i,d}\right)^T, \ldots\right]^T,\ d = 5D, 7.5D, 10D \tag{7}$$

Table 1. Wind turbine operating conditions for all performed tests with mod-TI and high-TI inflow conditions.

mod-TI, $U_0 = 5.60$ m/s					high-TI, $U_0 = 5.46$ m/s				
$\Omega[rpm]$	$\beta[°]$	$\gamma[°]$	$C_T[-]$	ID	$\Omega[rpm]$	$\beta[°]$	$\gamma[°]$	$C_T[-]$	ID
806.3	1.42	0	0.79	1	770.6	1.45	0	0.79	12
806.0	1.99	0	0.73	2	773.3	2.05	0	0.73	13
796.1	2.50	0	0.68	3	770.0	2.44	0	0.69	14
656.4	1.42	−40	0.51	4	631.2	1.42	−40	0.51	15
729.4	1.42	−30	0.63	5	693.2	1.42	−30	0.62	16
773.2	1.42	−20	0.72	6	734.8	1.42	−20	0.72	17
798.4	1.42	−10	0.77	7	758.5	1.43	−10	0.77	18
797.6	1.42	10	0.77	8	760.9	1.43	10	0.77	19
774.9	1.42	20	0.71	9	737.8	1.42	20	0.72	20
731.9	1.42	30	0.62	10	696.2	1.42	30	0.62	21
659.4	1.42	40	0.51	11	629.6	1.42	40	0.51	22

where $\hat{\boldsymbol{v}}^{i,d}$ and $\hat{\boldsymbol{t}}^{i,d}$ are respectively the normalized velocities and turbulence intensities predicted by a model at a downwind distance d and at the same points were the flow was measured during the experimental campaign.

The tuning process was then carried out in two steps, both requiring the minimization of a cost function, which was performed using MATLAB's `fminsearch`. At first, the adopted cost function (SRE) was defined as

$$SRE = \sum_{i=1}^{M} \sum_{d} \left[w_v \sum_{j=1}^{N^{i,d}} \left(\frac{\hat{v}_j^{i,d} - \tilde{v}_j^{i,d}}{\tilde{v}_j^{i,d}} \right)^2 + w_t \sum_{j=1}^{N^{i,d}} \left(\frac{\hat{t}_j^{i,d} - \tilde{t}_j^{i,d}}{\tilde{t}_j^{i,d}} \right)^2 \right], \tag{8}$$

where M is the number of used observations, $N^{i,d}$ is the number of data points measured, for the i^{th} observation, at the downwind distance d, while w_v and w_t are weighting factors. The output of the minimization problem was then used as initial guess for a successive minimization that seeks for a maximum likelihood estimate (MLE) of the models' tunable parameters, an approach that can account for the inevitable presence of various sources of errors and noise in the measurements. To this aim, the adopted cost function was defined, as in [17], equal to

$$J = \frac{Mn}{2} \ln(2\pi) + \frac{M}{2} \ln \det(\boldsymbol{R}) + \frac{1}{2} \sum_{i=1}^{M} \boldsymbol{r}_i^T \boldsymbol{R}^{-1} \boldsymbol{r}_i, \tag{9}$$

where $\boldsymbol{R}$, the error covariance matrix of the residuals computed as

$$\boldsymbol{R} = \frac{1}{M} \sum_{i=1}^{M} \boldsymbol{r}_i \boldsymbol{r}_i^T, \tag{10}$$

is nonsingular if M, the dimension of the residual vector $\boldsymbol{r}$, is smaller than the number of used observations M. In this regard, the residual $\boldsymbol{r}_i$ associated to the i^{th} observation was defined as

$$\boldsymbol{r}_i = \left[\ldots, w_v \left\| \left(\frac{\hat{\boldsymbol{v}}^{i,d} - \tilde{\boldsymbol{v}}^{i,d}}{\tilde{\boldsymbol{v}}^{i,d}} \right) \right\| + \sqrt{w_t} f^{i,d} \left(\hat{\boldsymbol{t}}^{i,d}, \tilde{\boldsymbol{t}}^{i,d} \right), \ldots \right]^T \quad d = 5D, 7.5D, 10D, \tag{11}$$

where the function $f^{i,d}$ was defined as $f^{i,d} = \frac{\overline{\hat{\boldsymbol{t}}^{i,d}} - \overline{\tilde{\boldsymbol{t}}^{i,d}}}{\overline{\tilde{\boldsymbol{t}}^{i,d}}}$ when tuning the Porté-Agel model's parameters, while it was defined as $f^{i,d} = \left\| \left(\frac{\hat{\boldsymbol{t}}^{i,d} - \tilde{\boldsymbol{t}}^{i,d}}{\tilde{\boldsymbol{t}}^{i,d}} \right) \right\|$ when tuning the 2D_k Jensen and Jensen-Gaussian models, with $\overline{\hat{\boldsymbol{t}}^{i,d}}$ and $\overline{\tilde{\boldsymbol{t}}^{i,d}}$ respectively the predicted and measured average turbulence within the wake at a distance d.

5. Results

In order to account for the different capabilities of the the various investigated models, different set of observations were used for their parameters' tuning. Moreover, since it is well-known that the inflow turbulence strongly affect the wake decay rate [18], two distinguished set of parameters were tuned using, separately, observations performed with mod-TI and high-TI inflows. However, only a single set of the Porté-Agel model's parameters was tuned, using observations pertaining to both inflows. This model, indeed, already accounts, through Eq. 4c, for the relationship between the inflow turbulence and the wake recovery. Despite the 2D_k Jensen and Jensen-Gaussian models also account for this relationship (Eqs. 5a and 6a), preliminary verifications showed that a single set of tunable parameters would have provided poor predictions of the speed in the wake.

Table 2. Models' tuned parameters.

	mod-TI			high-TI		
Jensen	$\alpha = 0.033$			$\alpha = 0.047$		
Frandsen	$\alpha_{(noj)} = 0.008$	$k = 3.023$		$\alpha_{(noj)} = 0.020$	$k = 1.740$	
FLORIS	$M_{U,1} = 0.227$ $m_{e,1} = -0.694$ $k_d = 0.105$ $a_U = 13.551$	$M_{U,2} = 0.719$ $m_{e,2} = 0.369$ $a_d = -0.071$ $b_U = -0.112$	$M_{U,3} = 2.341$ $m_{e,3} = 0.876$ $b_d = 0.014$	$M_{U,1} = 0.388$ $m_{e,1} = -0.646$ $k_d = 0.168$ $a_U = 7.666$	$M_{U,2} = 0.692$ $m_{e,2} = 0.250$ $a_d = -0.077$ $b_U = 0.040$	$M_{U,3} = 1.809$ $m_{e,3} = 1.097$ $b_d = 0.011$
2D_k Jensen	$k_0 = 0.0343$	$TI_a = 0.1252$	$TI_b = -0.0287$	$k_0 = 0.0524$	$TI_a = 0.3624$	$TI_b = -0.5998$
Jensen-Gaus.	$k_0 = 0.0307$	$Kn = 0.2628$		$k_0 = 0.0879$	$Kn = 0.141$	
Porté-Agel	$k_a = 0.089$, $k_b = 0.027$, $\alpha = 0.952$, $\beta = 0.262$, $TI_a = 0.082$, $TI_b = 0.608$, $TI_c = -0.551$, $TI_d = -0.277$					

The parameters of the Jensen, Frandsen, 2D_k Jensen and Jensen-Gaussian models were calibrated using observations obtained with the aligned wind turbine rotor (ID 1-3 for mod-TI, ID 12-14 for high-TI, see Table 1). Concerning the FLORIS model, the parameters that govern the wake deficit were tuned first using the non-yawed cases, while the parameters that govern the wake deflection were tuned after, using the observations gathered with a misaligned wind turbine (ID 1/4-11 for mod-TI, ID 12/15-22 for high-TI). Concerning the weighting factors w_v and w_t of Eqs. 8 and 11, they were set respectively equal to 1 and 0 when tuning the parameters of those models that do not provide sub-models for the turbulence intensity prediction, while they were set respectively equal to 1 and 0.1 when tuning the parameters of the 2D_k Jensen and Jensen-Gaussian models. These two models, indeed, make use of prediction of the turbulence intensity within the wake to estimate its deficit; an higher value of w_v was then used to guide the optimizer toward the research of a set of parameters that provide a better estimation of the wake velocity deficit, rather than a proper estimation of its turbulence intensity. Concerning the tuning of the parameters of the Porté-Agel model, those that govern the wake deficit/deflection were tuned first, setting $w_v = 1$ and $w_t = 0$, and using all observations except the ones with $\gamma = \pm 40°$. Successively, the parameters of the turbulence sub-models were tuned, setting $w_v = 0$ and $w_t = 1$, and using observations obtained with the aligned wind turbine rotor. The resulting tuned parameters are reported in Table 2.

5.1. Comparison between experiments and models' predictions

Figures 1 and 2 depict the models' predicted normalized flow velocity and the corresponding measurement data for the non-yawed cases, and for moderate and high turbulence intensity inflow conditions, respectively.

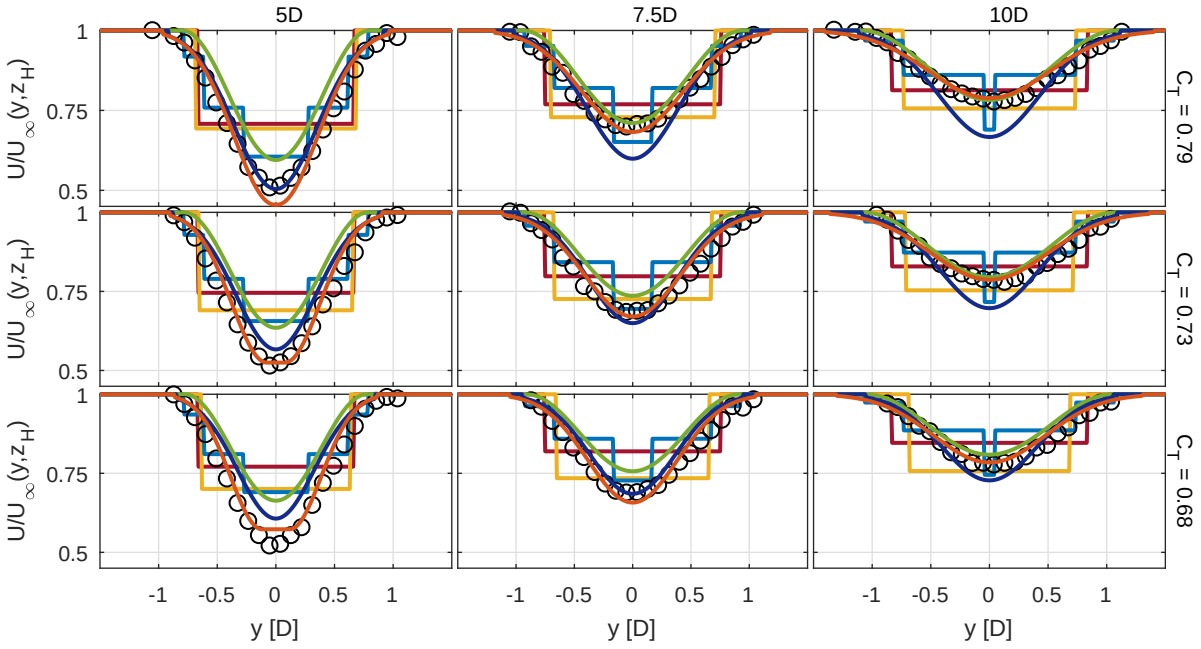

Figure 1. Flow velocity estimations for the Jensen (—), Frandsen (—), FLORIS (—), 2D_k Jensen (—), Jensen-Gaussian (—) and Porté-Agel (—) models compared to wind tunnel measurements (○) performed at hub height, with mod-TI inflow, null yaw misalignment and three C_T settings (ID 1-3).

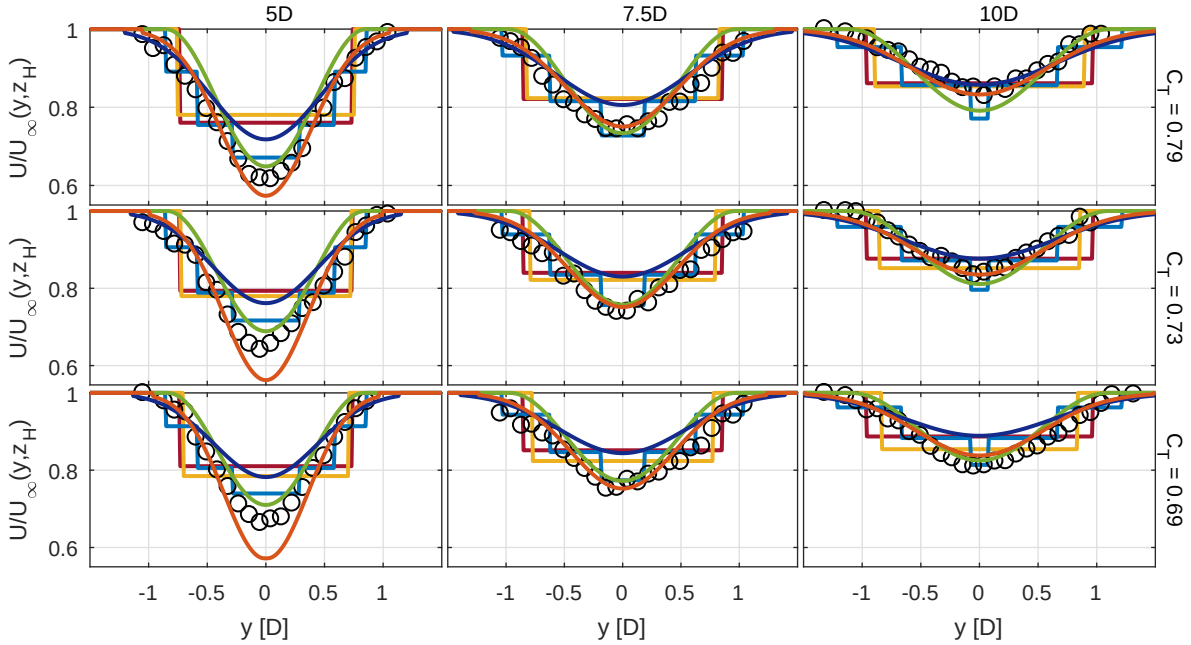

Figure 2. Flow velocity estimations for the Jensen (—), Frandsen (—), FLORIS (—), 2D_k Jensen (—), Jensen-Gaussian (—) and Porté-Agel (—) models compared to wind tunnel measurements (○) performed at hub height, with high-TI inflow, null yaw misalignment and three C_T settings (ID 12-14).

The plots highlight that the Jensen and Frandsen models' predictions are quite inaccurate, especially for mod-TI inflow, while the predictions of the other models are quite satisfactory, particularly for high-TI inflow. Quite outstanding are the wind speed estimations of the Porté-Agel model, especially for mod-TI inflow conditions, while it seems that the same model is overestimating the wake deficit at 5D for high-TI inflow and with the wind turbine operating under de-rated power conditions.

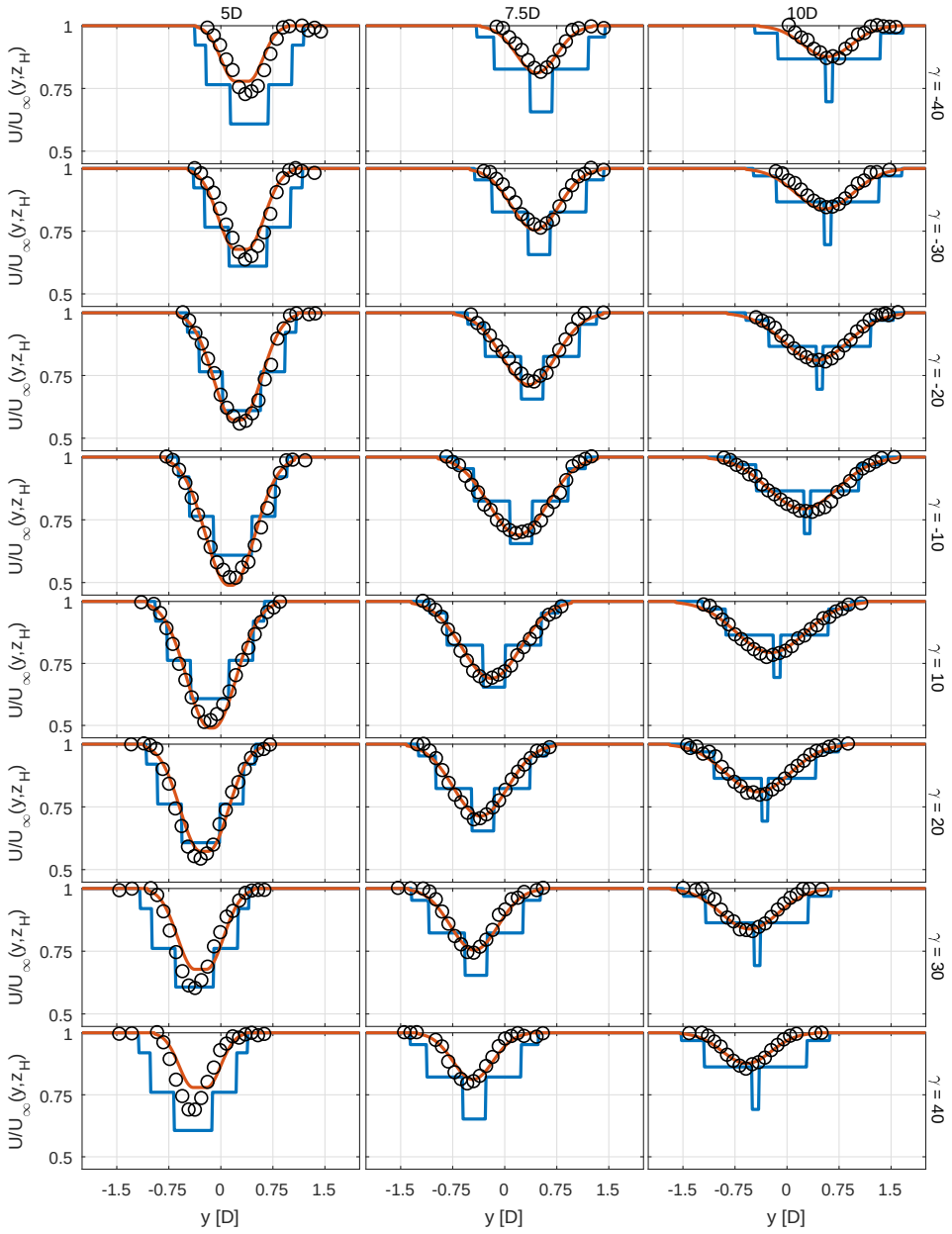

Figure 3. Flow velocity estimations for the FLORIS (—) and Porté-Agel (—) models compared to wind tunnel measurements (○) performed at hub height, mod-TI inflow, γ = -40:10:-10 & 10:10:40 (ID 4-11).

Since only the FLORIS and Porté-Agel models are capable of predicting the wake deflection

due to yaw-misaligned conditions, Figs. 3 and 4 report, respectively for mod-TI and high-TI inflow conditions, the comparison between the experimental data and the normalized wake speed estimated by these two models when the G1 was yawed of $\gamma = \pm 40, \pm 30, \pm 20, \pm 10$.

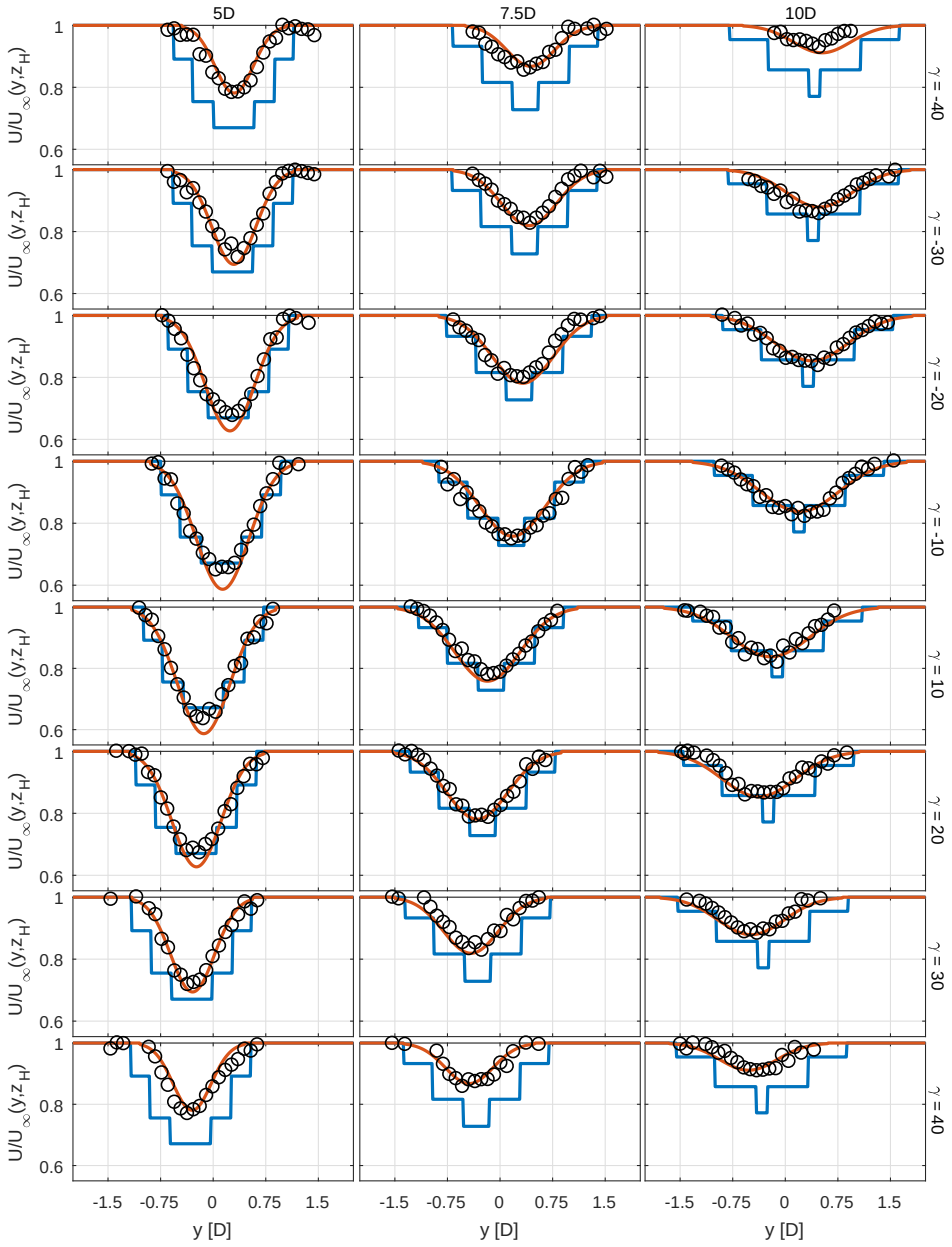

Figure 4. Flow velocity estimations for the FLORIS (—) and Porté-Agel (—) models compared to wind tunnel measurements (○) performed at hub height, high-TI inflow, γ = -40:10:-10 & 10:10:40 (ID 15-22).

The plots within the figures allow to appreciate the impact of yaw misaligned operations on the wake shed by the scaled wind turbine model: as expected, as higher the misalignment is, as lower is the wake velocity deficit and higher is the wake deflection. Concerning the models' predictions, both the FLORIS and Porté-Agel are quite accurate, specially for γ between the

range of ±20°. The FLORIS model seems however less accurate for $\gamma = \pm 30°$, and quite inaccurate for those conditions characterized by very high yaw misalignment, i.e with $\gamma = \pm 40°$. The Porté-Agel's prediction are overall outstanding, despite a moderate mismatch with the experimental observations can be observed for $\gamma = \pm 40°$ and mod-TI inflow conditions.

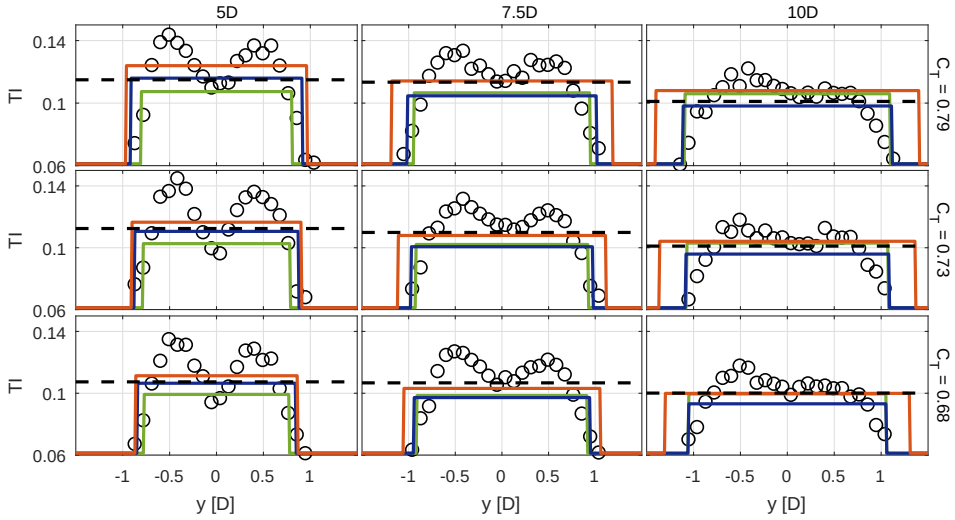

Figure 5. Turbulence intensity estimations for the 2D_k Jensen (—), Jensen-Gaussian (—) and Porté-Agel (—) models compared to wind tunnel measurements (○) performed at hub height, with mod-TI inflow, null yaw misalignment and three C_T settings (ID 1-3). The experimental average turbulence intensity within the wake is reported with a black dashed line.

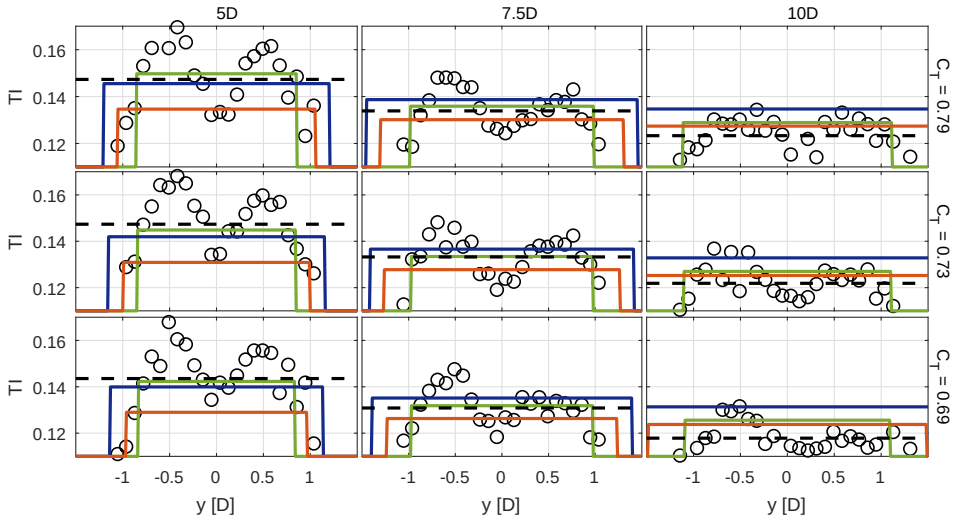

Figure 6. Turbulence intensity estimations for the 2D_k Jensen (—), Jensen-Gaussian (—) and Porté-Agel (—) models compared to wind tunnel measurements (○) performed at hub height, with high-TI inflow, null yaw misalignment and three C_T settings (ID 12-14). The experimental average turbulence intensity within the wake is reported with a black dashed line.

Three of the investigated models (2D_k Jensen, Jensen-Gaussian and Porté-Agel) are also

capable of estimating the turbulence intensity within the wake. These are compared to the experimental observations in Figs. 5 and 6. Since all models assume a spatially constant turbulence, they are not capable of correctly reproducing the distribution of the turbulence along the horizontal line. In any case, it is possible to evaluate the accuracy of the three models in predicting the average value of the wake turbulence, whose experimental data is also reported in the subplots. In this sense, all three models produce satisfactory estimates for low-TI inflow, with the Porté-Agel model that seems to perform slightly better than the others. However, the data related to the high-TI inflow show that the 2D_k Jensen model is more effective than the other two in predicting the wake turbulence at 5D, while predictions for greater distances tend to get closer. It seems, in fact, that the Jensen-Gaussian and Porté-Agel models are not able to properly estimate the rate of decrease of the turbulence in the wake associated with its speed recovery.

5.2. Overall assessment of the models' accuracy

In order to quantitatively assess the average accuracy of the investigated models, in terms of prediction of the wake speed, deflection and turbulence intensity for all tested conditions, three average Root Mean Squared Relative Error (RMSRE) were calculated as

$$\mathrm{RMSRE}_v = \frac{1}{M}\sum_{i=1}^{M}\sqrt{\frac{1}{3}\sum_{d}\frac{1}{N^{i,d}}\sum_{j=1}^{N^{i,d}}\left(\frac{\hat{v}_j^{i,d}-\tilde{v}_j^{i,d}}{\tilde{v}_j^{i,d}}\right)^2}, \tag{12a}$$

$$\mathrm{RMSRE}_t = \frac{1}{M}\sum_{i=1}^{M}\sqrt{\frac{1}{3}\sum_{d}\left(\frac{\overline{\hat{\boldsymbol{t}}^{i,d}}-\overline{\tilde{\boldsymbol{t}}^{i,d}}}{\overline{\tilde{\boldsymbol{t}}^{i,d}}}\right)^2}. \tag{12b}$$

In particular, six RMSRE_v were computed, for all models, using prediction and observations related to all the non-yawed cases. Similarly, two RMSRE_v were computed, for the FLORIS and Porté-Agel models, using prediction and observations related to all the yawed cases. Finally, three RMSRE_t were computed using data related to all the non-yawed cases.

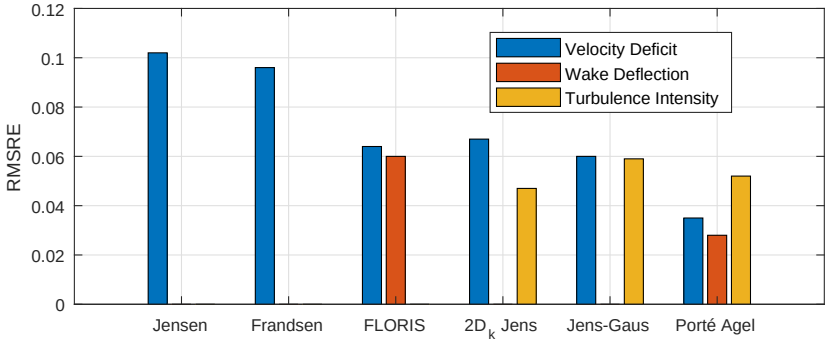

Figure 7. Average RMSRE of model estimations for velocity deficit, wake deflection and turbulence intensity.

The obtained RMSRE, reported in Fig. 7, confirm the observations discussed in the previous section. The Porté-Agel model, indeed, provide the best predictions of the velocity deficit and wake deflection. However, different conclusions can be given by looking at the accuracy of the turbulence intensity predictions: in this case, indeed, the 2D_k Jensen model exhibits the best performance.

6. Conclusions and outlook

The comparison between the experimental data and the numerical predictions, as well as the overall evaluation of the accuracy of the various models, allows to conclude that the Porté-Agel model seems to be the most accurate in terms of prediction of the wake speed and deflection related to a wide range of inflow and wind turbine operating conditions (thrust coefficient and yaw misalignment). Moreover, the model tuning requires the identification of solely four parameters, i.e. less than all the other models except the Jensen-Gaussian, which, however, do not provide estimation of the wake deflection.

However, further improvements could still be added to the model. One of this could be accounting, as suggested by [19], for the dependency of the wake decay rate to the operating thrust coefficient by modifying Eq. 4c into

$$k_y = k_z = \boldsymbol{k_a} I_0 + \boldsymbol{k_b} + \boldsymbol{k_c} C_T. \tag{13}$$

By utilizing this approach, a new set of parameters (k_a =0.054, k_b=0.025, k_c=0.003, α=1.642, β=0.155) can be found, leading to a reduction, from 0.0350 to 0.0281, of the RMSRE_v related to all the non-yawed cases. Finally, another minor improvement to the Porté-Agel would be the implementation of a difference turbulence intensity sub-model, like the one of 2D_k Jensen model. A better prediction of the turbulence in the wake would lead, in fact, to a better prediction of the recovery associated to a wake shed by a downstream turbine.

Acknowledgments

This work has been supported by the CL-WINDCON project, which receives funding from the European Union Horizon 2020 research and innovation program under grant agreement No. 727477.

References

[1] Knudsen T, Bak T and Svenstrup M 2015 *Wind Energy* **18** 1333-1351
[2] Jensen, N O 1983 A note on wind generator interaction
[3] Frandsen, S, Barthelmie, R, Pryor, S, Rathmann, O, Larsen, S, Hjstrup, J, and Thgersen, M (2006). *Wind Energy: An International Journal for Progress and Applications in Wind Power Conversion Technology* **9(12)** 39-53
[4] Gebraad, P M, Teeuwisse, F W, Van Wingerden, J W, Fleming, P A, Ruben, S D, Marden, J R, and Pao, L Y 2014 *In American Control Conference (ACC)* 3128-3134
[5] Tian, L, Zhu, W, Shen, W, Zhao, N, and Shen, Z 2015 *Journal of Wind Engineering and Industrial Aerodynamics*, **137** 90-99
[6] Tian, L, Zhu, W, Shen, W, Song, Y, and Zhao, N 2017 *Renewable Energy* **102** 457-46
[7] Larsen, G C, Højstrup, J, and Madsen, H A 1996 *EWEC 1996 Proceedings*
[8] Gao, X, Yang, H, and Lu, L 2016 *Applied Energy* **174** 192-200
[9] Bastankhah, M, and Porté-Agel, F 2014 *Renewable Energy* **70** 116-123
[10] Niayifar, A, and Porté-Agel, F 2015 *J. Phys. Conf. Seri.* **625** 012039
[11] Bastankhah, M, and Porté-Agel, F 2016 *Journal of Fluid Mechanics* **806** 506-541
[12] Crespo, A, and Herna, J 1996 *Journal of wind engineering and industrial aerodynamics* **61(1)** 71-85
[13] Campagnolo F, Petrović, V, Schreiber, J, Nanos, E M and Bottasso, C L 2016 *J. Phys. Conf. Seri.* **753**(3) 032006
[14] Bottasso, C L, Cacciola, S, and Iriarte, X 2014 *Journal of wind engineering and industrial aerodynamics* **124** 2945.
[15] Bottasso, C L, Campagnolo, F and Petrović, V 2014 *Journal of wind engineering and industrial aerodynamics* **127** 1128.
[16] Wang, J, Foley, S, Nanos, E, Yu, T, Campagnolo, F, Bottasso, C, Zanotti, A, and Croce, A 2017 *J. Phys. Conf. Ser.* **854** 012048
[17] Jategaonkar, R V 2015 *American Institute of Aeronautics and Astronautics, Inc.*
[18] Göçmen, T, Van der Laan, P, Réthoré, P-E, Diaz, A P, Larsen, G C, and Ott, S 2016 *Renewable and Sustainable Energy Reviews* **60** 752769
[19] Campagnolo, F, Petrović, V, Bottasso, C L and Croce, A 2016 *In American Control Conference (ACC)* 513-518